Laser and Particle Beams (2007), *25*, 365–370. Printed in the USA.

DOI: 10.1017/S0263034607000237

Bifurcating energy-angular spectrum of electrons accelerated by intense laser pulse

D. LIN,[1] Y.K. HO,[1] Q. KONG,[1] Z. CHEN,[1] P.X. WANG,[1] J.J. XU,[1] AND S. KAWATA[2]
[1]The Key Laboratory of Applied Ion Beam Physics, Institute of Modern Physics, Fudan University, Shanghai, China
[2]Department of Electrical and Electronic Engineering, Utsunomiya University, Utsunomiya, Japan

(RECEIVED 16 March 2007; ACCEPTED 20 April 2007)

Abstract

Bifurcation phenomenon in the energy-angular correlation spectrum of the vacuum laser acceleration has been observed with computer simulation. Concerning a focused laser pulse, the classical single-valued energy-angular correlation spectrum for a plane wave is, besides broadened to a band, bifurcated with the classical value in between the two branches. Analytic expression to describe the correlation has been derived and physical explanations based on the ponderomotive potential model and Lorentz-Newton force analyses are presented. The theoretical results are supported by numerical simulations which have been compared with the experimental results. This study is helpful in designing vacuum laser acceleration experiments.

Keywords: Electron dynamics in laser field; Energy-angular correlation; Laser acceleration

1. INTRODUCTION

Rapid development of laser technology has excited a lot of interest in studying the interactions of ultra intense lasers with matters (Fuchs *et al.*, 2006; Leemans *et al.*, 2006; Mourou *et al.*, 2006). Laser acceleration of charged particles is one of these research subjects (Pang *et al.*, 2002; Shorokhov & Pukhov, 2004; Glinec *et al.*, 2005; Roth *et al.*, 2005; Brambrink *et al.*, 2006; Lifschitz *et al.*, 2006; Mangles *et al.*, 2006; Yin *et al.*, 2006). Among the plenty of proposed acceleration schemes, ponderomotive acceleration (Quesnel & Mora, 1998; Badziak *et al.*, 2005) is one which has been demonstrated by the experiments producing MeV electrons in a vacuum (Malka *et al.*, 1997). Normally, the ponderomotive acceleration refers to an interaction scenario where an intense laser pulse catches non-relativistic free electrons in the focal region, then interacts, and accelerates the electrons. According to the theoretical predictions as well as the experimental results (Malka *et al.*, 1997), there exists a strong energy-angular correlation for the accelerated electrons.

In this paper, we present an interesting phenomenon observed with computer simulation in the vacuum laser ponderomotive acceleration, where the energy-angular correlation spectrum is bifurcated at high energy, while for plane wave acceleration, the correlation reduces to single-valued function. Physical explanation will also be addressed. This study may provide useful information for better understanding of the physics behind the ponderomotive acceleration, and for designing vacuum laser acceleration experiments.

Address Correspondence and reprint requests from: Y. K. Ho, Fudan University, Institute of Modern Physics, Handan Road 220, 200433, Shanghai, China. E-mail: hoyk@fudan.edu.cn

2. THEORETICAL ANALYSES

From the ponderomotive potential model (Kibble, 1966), when a free electron moves in a laser pulse, the electron experiences a time-averaged force, namely the ponderomotive force which is given by $F_{pond} = -\nabla V_{pond}(r,z,t)$, where V_{pond} is the ponderomotive potential $V_{pond} = (\sqrt{1+|a(r,z,t)|^2/2}-1)m_e c^2$, and $a(r,z,t) = eE/m\omega c$ is a dimensionless parameter measuring the laser intensity. Accordingly, the transverse and longitudinal ponderomotive forces of a TEM (0, 0) mode laser propagating along the z axis can be derived as below (Kawata *et al.*, 2005):

$$F_r = \frac{a^2 r}{w_z^2\sqrt{1+a^2/2}},$$
$$F_z = \frac{a^2}{\sqrt{1+a^2/2}}\left[\frac{2z}{w_0^2 w_z^2}\left(1-\frac{2r^2}{w_z^2}\right)+\frac{\eta}{\tau^2}\right], \quad (1)$$

$$a = \frac{E_0}{mc\omega}\frac{w_0}{w_z}\exp\left(-\frac{r^2}{w_z^2}\right)\exp\left(-\frac{\eta^2}{\tau^2}\right), \quad (2)$$

where $r = \sqrt{x^2 + y^2}$, $\eta = z - ct$, and $w_z = w_0[1 + (2z/kw_0^2)^2]^{1/2}$. The spot size, the wave number and the pulse duration are w_0, k, and τ, respectively.

The transverse ponderomotive force F_r is always positive, it means the off-axis electrons can be accelerated and scattered transversely by the ponderomotive potential. As for the longitudinal ponderomotive force F_z, there are two components which represent two different sources for the electron energy change. The former term $(1 - 2r^2/w_z^2)2z/w_0^2w_z^2$ comes from the radial gradient of the laser intensity, namely the diffraction effect of the focused laser. The latter one η/τ^2 comes from the intensity gradient of the laser pulse, namely the effect of the finite pulse duration. Here η represents the relative distance between the electron and the laser pulse center. A schematic explanation of the ponderomotive acceleration is that interaction with the laser ascending front (climbing hill) corresponds to acceleration, whereas with the laser descending part (downhill) for deceleration. When a laser pulse catches an electron in the focal region, the intensity experienced by the electron in the ascending front is higher than that in the descending part owing to the diffraction effect of the focused laser. As a result, the electron can gain net energy in the interaction process.

The ponderomotive acceleration scheme has been demonstrated by experiments producing electrons of MeV energies in a vacuum (Malka *et al.*, 1997). The spectrometer is set at certain observation angles. Hence, it is of interest to study the properties of the vacuum laser ponderomotive acceleration, especially the correlation between the outgoing energy, and the scattering angle of the accelerated electrons.

The energy-momentum transfer equations are written:

$$\frac{d(\gamma\boldsymbol{\beta})}{dt} = \frac{-e}{m_0c}(\mathbf{E} + c\boldsymbol{\beta} \times \mathbf{B}), \quad (3)$$

$$\frac{d\gamma}{dt} = \frac{-e}{m_0c}\boldsymbol{\beta} \cdot \mathbf{E}, \quad (4)$$

where e, m_0, and $\boldsymbol{\beta}$ are, respectively, the charge, mass, and normalized velocity of the electron, γ is the Lorentz factor, $\mathbf{E}$ and $\mathbf{B}$ are the electric and magnetic field.

Considering a planar electromagnetic wave propagating along the z axis, the z component of Eq. (3) can be written as:

$$\frac{d(\gamma\beta_z)}{dt} = \frac{-e}{m_0c}\boldsymbol{\beta} \cdot \mathbf{E}. \quad (5)$$

Combining Eqs. (4) and (5), one can get the invariant

$$d[\gamma(1 - \beta_z)]/dt = 0, \quad (6)$$

thus, $\gamma(1 - \beta_z) = \gamma_0(1 - \beta_{z0})$, where the subscript zero refers to the initial value, and we get the single-valued function of the energy-angular correlation (Salamin & Faisal, 1997; Hartemann & Kerman, 2001):

$$\tan\theta_p = \frac{\beta_\perp}{\beta_z} = \frac{\sqrt{2\gamma\gamma_0(1 - \beta_{z0}) - \gamma_0^2(1 - \beta_{z0})^2 - 1}}{\gamma - \gamma_0(1 - \beta_{z0})}. \quad (7)$$

However, as for a focused laser pulse, the above single-valued function is no longer applicable. Assuming the laser pulse can be described by using the paraxial approximation to a Gaussian beam (Moore *et al.*, 2001), the z component of Eq. (3) is changed to (Chen *et al.*, 2004):

$$\frac{d(\gamma\beta_z)}{dt} = \frac{-e}{m_0c}[(1 - \beta_z)E_z + \boldsymbol{\beta} \cdot \mathbf{E}]. \quad (8)$$

Thus we get:

$$\frac{d[\gamma(1 - \beta_z)]}{dt} = \frac{e}{m_0c}(1 - \beta_z)E_z. \quad (9)$$

Comparing Eq. (9) with Eq. (6), we can find the difference between the focused laser pulse and the plane wave consists in the item of E_z. For a laser pulse with finite width, $\gamma(1 - \beta_z)$ will not be invariant since $E_z \neq 0$.

3. SIMULATION RESULTS AND DISCUSSIONS

Then we resort to numerical analyses based on Lorentz-Newton Eqs. (3) and (4). We present a typical case for a non-relativistic electron bunch accelerated by a Hermite–Gaussian (0, 0)-mode laser pulse. The cylinder bunch of electrons is injected from minus z direction with the initial velocity of $\beta_{z0} = 0.1$, while $\beta_{x0} = \beta_{y0} = 0$, and the electrons are assumed to distribute uniformly. The transverse size of the bunch is the same as the laser beam width at focus w_0, and the longitudinal size is the Rayleigh length $Z_R = kw_0^2/2$. Without losing generality, we assume that the laser pulse center reaches the point $x = y = z = 0$ at time $t = 0$, and that the center of the electron bunch is incident with a certain initial position z_0 chosen so as to arrive at $x = y = z = 0$ at time $t = 0$ under the condition of free motion. Also, we define the relative initial longitudinal position ΔZ_0 of an electron as the distance between the initial position of the electron and that of the bunch center.

Figure 1 presents a comparison of the theoretical calculations based on Eq. (9) and the simulations for the correlation between the outgoing energy and the scattering angle. One can see that the classical single-valued energy-angular correlation for plane wave is, not only broadened to a band which means electrons with the same outgoing energy will have an angular spread, but bifurcated at high energy with the classical value in between the two branches as well.

https://doi.org/10.1017/S0263034607000237 Published online by Cambridge University Press

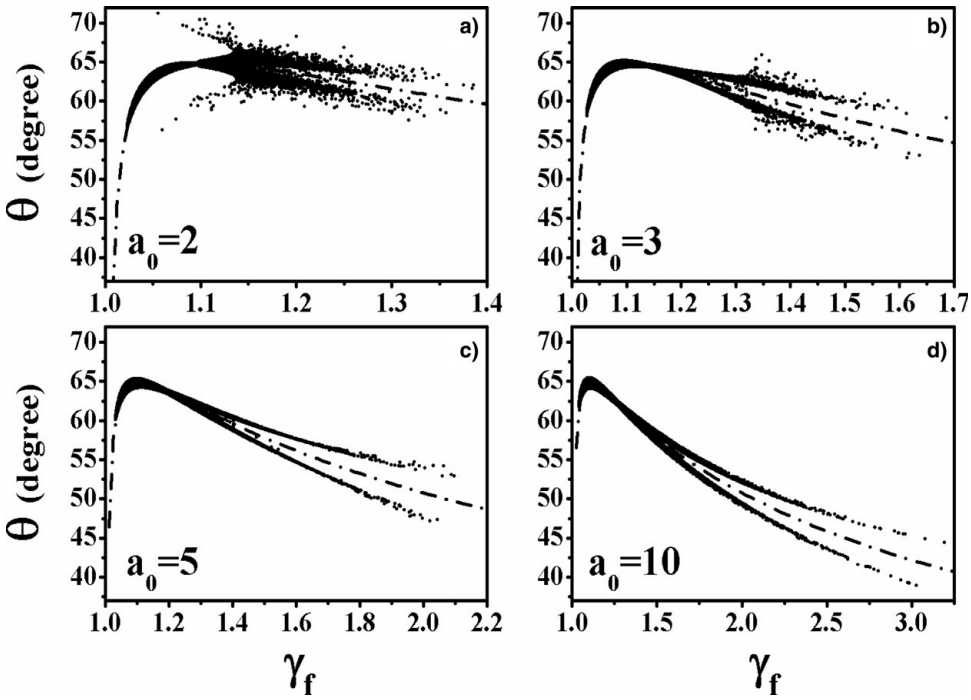

Fig. 1. The correlation between the outgoing energy and the scattering angle at different laser intensities. A linear polarized TEM_{00} Gaussian laser pulse with pulse duration $\omega\tau = 550$ is used. The initial momentum of the electrons is $p_{x0} = p_{y0} = 0$, and $p_{z0} = 0.1$ which are normalized by m_0c. The black spot is for the simulation result, while the red solid line is for the calculated energy-angular correlation under the plane wave condition. (**a**) For $a_0 = 2$, and (**b**), (**c**), (**d**) for $a_0 = 3$, 5, 10, respectively.

Now we go on to explain the interesting splitting phenomenon in the energy-angular correlation observed from the simulations. From Eq. (9) we get:

$$\gamma(1-\beta_z) = \int_0^t \frac{e}{m_0 c}(1-\beta_z)E_z dt + \gamma_0(1-\beta_{z0}) \equiv \Delta_T + N, \quad (10)$$

where

$$\Delta_T = \int_0^t \frac{e}{m_0 c}(1-\beta_z)E_z dt,$$

and

$$N = \gamma_0(1-\beta_{z0}),$$

thus

$$\tan\theta = \frac{\beta_\perp}{\beta_z} = \frac{\sqrt{2\gamma\gamma(1-\beta_z) - \gamma^2(1-\beta_z)^2 - 1}}{\gamma - \gamma_0(1-\beta_{z0}) - \Delta_T}. \quad (11)$$

Comparing with the correlation of the plane wave $\tan\theta_p$, we get:

$$\tan^2\theta - \tan^2\theta_p = (\tan^2\theta_p + 1)\left[\left(\frac{\gamma - N}{\gamma - N - \Delta_T}\right)^2 - 1\right]. \quad (12)$$

From Eq. (12), one may find that when

$$\left(\frac{\gamma - N}{\gamma - N - \Delta_T}\right)^2 - 1 > 0, \tan^2\theta - \tan^2\theta_p > 0,$$

whereas

$$\left(\frac{\gamma - N}{\gamma - N - \Delta_T}\right)^2 - 1 < 0, \tan^2\theta - \tan^2\theta_p < 0.$$

Also, we have $\Delta_T < 2(\gamma - N)$, accordingly we get that whether the value of $\tan^2\theta$ is lager than $\tan^2\theta_p$ depends on the sign of Δ_T. In fact, $\Delta_T = \gamma(1-\beta_z) - N = \Delta\gamma - \Delta p_z$, which means that Δ_T measures the transverse momentum change of the electron. The simulation results for the correlation between the scattering angle and Δ_T is presented in Figures 2a and 2b, which is consistent with the above analysis, that when $\Delta_T > 0$, $\tan\theta > \tan\theta_p$, whereas $\Delta_T < 0$, $\tan\theta < \tan\theta_p$.

Still, we investigate a typical case with laser intensity $a_0 = 5$. Figure 2c gives the output energy γ_f versus the relative initial longitudinal position ΔZ_0 of the electrons. Comparing the simulated energy–angular correlation of the laser pulse with the calculated value of the plane wave (Fig. 2d), one may find that the two bifurcated branches at high energy stem from electrons with different initial longitudinal positions. An electron which initially locates ahead of the center of the electron bunch ($\Delta Z_0 > 0$) will have a

https://doi.org/10.1017/S0263034607000237 Published online by Cambridge University Press

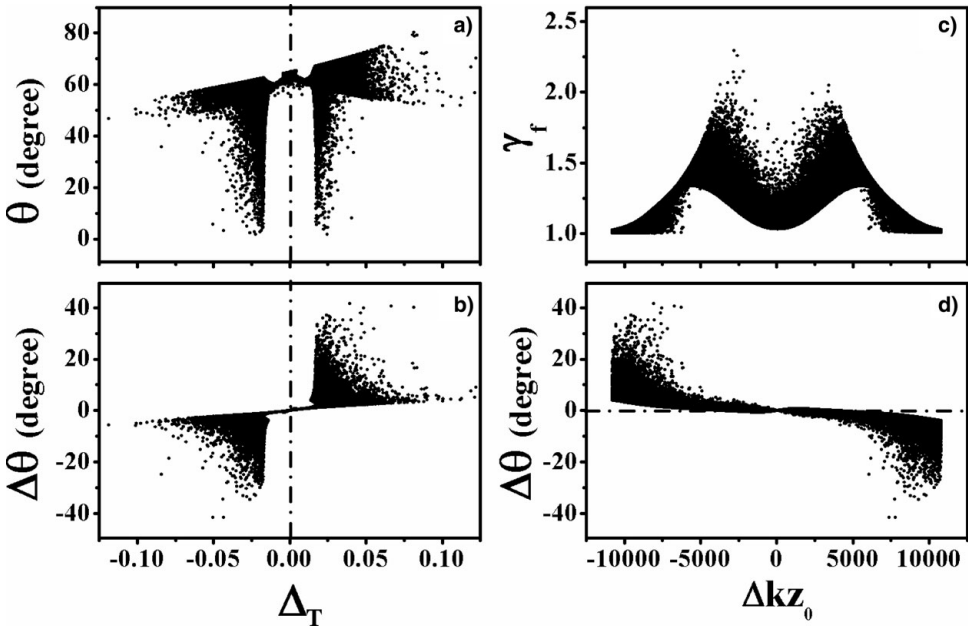

Fig. 2. Simulation results of electrons accelerated by vacuum laser pulse with intensity $a_0 = 5$. The other parameters used are the same as those in Figure 1. (**a**) Scattering angle as a function of Δ_T; (**b**) The difference between the scattering angle and the plane-wave value $\Delta\theta$ as a function of Δ_T; (**c**) Simulation results on the correlation between the outgoing energy and the electron relative initial longitudinal position ΔZ_0; (**d**) The difference between the scattering angle and the plane-wave value $\Delta\theta$ as a function of ΔZ_0.

scattering angle smaller than the calculated plane wave value; while an electron behind the electron bunch center ($\Delta Z_0 < 0$) will have a scattering angle larger than that of the plane wave. Here we define the former as leading electrons, while the latter as trailing electrons.

Figure 3 presents the detailed dynamics for two electrons selected respectively from the two branches with the same outgoing energy $\gamma_f = 2.25$. The scattering angles for the corresponding plane wave, the trailing electron, and the leading electron are 48.1°, 51.6°, and 44.6°, respectively. From Figure 3, one may find that the transverse momentum p_r of the trailing electron is larger than that of the leading one, while the longitudinal momentum p_z of the trailing electron is less than that of the leading one. Therefore, the branch with larger scattering angle corresponds to the trailing electrons, while the branch with smaller scattering angle is for the leading electrons.

From the ponderomotive force model, the electron scattering angle is

$$\tan\theta = \frac{p_r}{p_z} = \frac{\int \frac{w_0}{w_z}\exp\left(-\frac{r^2}{w_z^2}\right)\exp\left(-\frac{\eta^2}{\tau^2}\right)\frac{r}{w_z^2}\,dt}{\int \frac{w_0}{w_z}\exp\left(-\frac{r^2}{w_z^2}\right)\exp\left(-\frac{\eta^2}{\tau^2}\right)\left[\frac{2z}{w_0^2 w_z^2}\left(1-\frac{2r^2}{w_z^2}\right)+\frac{\eta}{\tau^2}\right]dt}. \quad (13)$$

The interaction feature of the trailing electrons with the laser pulse is quite different from that of the leading ones. The strong interaction for the trailing electron takes place mainly in the tapered region prior to the laser focus, whereas that for the leading electron is behind the focus in the inversely-tapered region. Thus the mean value of w_z for the trailing electron is less than that of the leading electron. Since the item w_z plays an important role in the numerator of Eq. (13), we can make a judgment that the transverse momentum p_r of the trailing electron will be larger than that of the leading one. As for the longitudinal momentum p_z, the "downhill" process of the trailing electron in the tapered interaction region will be stronger compared with that of the leading electron, therefore p_z of the trailing electron will be less than that of the leading one. In conclusion, the scattering angle of the trailing electron is larger than that of the leading one, which causes the bifurcating phenomenon and is consistent with the simulation results.

To make a comparison with experimental data, it should be noted that though the occurrence of the bifurcation is in common for any kind of laser beam profiles, however the detailed value of the scattering angle is related to the beam profile in someway. For instance, the scattering angle by flattened Gaussian beam will be smaller than that with relevant standard Gaussian beam. This point can easily be understood from the ponderomotive potential model. We simulated the parameters of Malka *et al.* (1997), which is the only experimental data available now on vacuum laser acceleration ($a_0 = 2$, *and* 3; $v_0 = 0.1c$, *and* $0.2c$). A general agreement has been found in terms of the maximum energies. The data presented in Malka *et al.* (1997) is not sufficient to make any judgment on whether or not there is bifurcation. And the calculated scattering angle based on the standard Gaussian model (Eqs. (1) and (2)) is somewhat larger than

https://doi.org/10.1017/S0263034607000237 Published online by Cambridge University Press

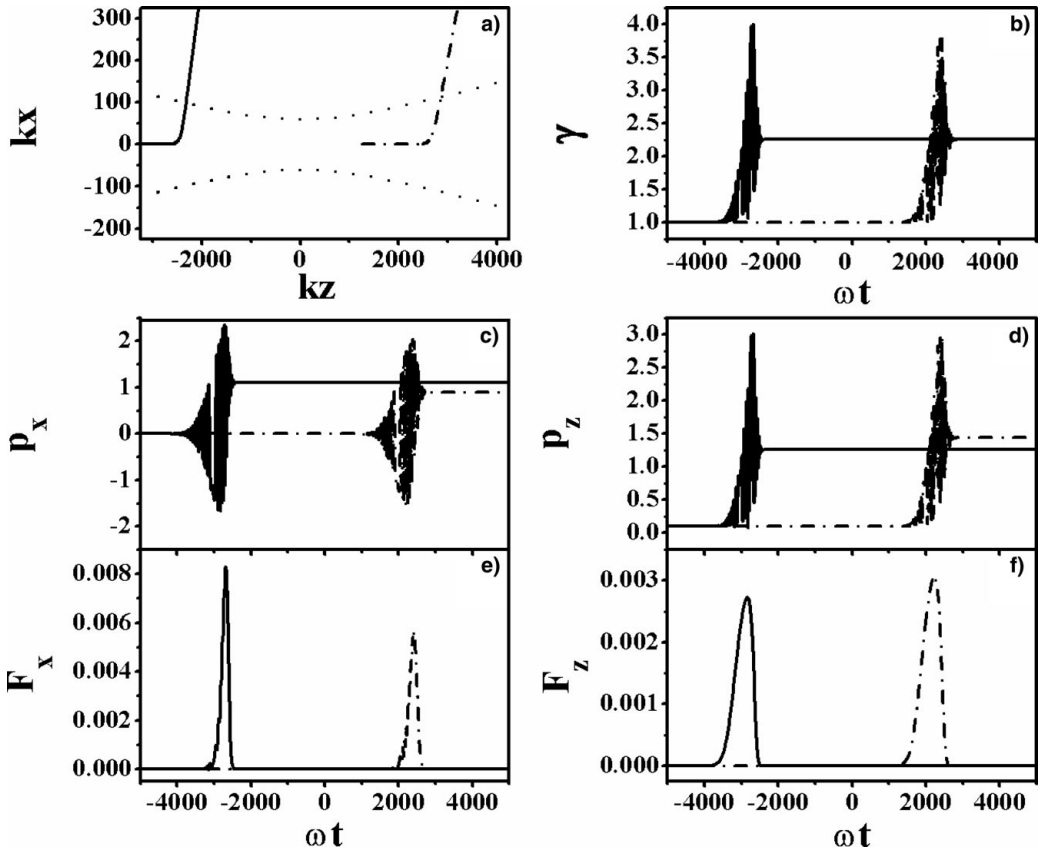

Fig. 3. The electron dynamics of a leading electron (the solid line) and a trailing electron (the dash dot line). These two electrons are selected from the electron bunch of Figure 2 with the same outgoing energy $\gamma_f = 2.25$ but different scattering angles (51.6° and 44.6°, respectively), therefore belong to different bifurcated branches. The parameters used are the same as in Figure 2. (**a**) The electron dynamic trajectories in x-z plane. The dashed lines denote the laser beam width $w(z)$. (**b**) The electron final energy γ vs. t. (**c**) and (**d**) The electron momentum in the x and z direction, respectively as functions of time. (**e**) and (**f**) The ponderomotive force experienced by the electron in the x and z direction, respectively, as functions of time.

the experimental data, it seems to mean that the profile of the laser beam utilized in the experiments of Malka *et al.* (1997) is close to a flattened Gaussian one.

4. SUMMARY

The energy-angular correlation of the outgoing electrons in laser-driven electron acceleration has been studied both analytically and numerically. For the first time, this paper reported the bifurcating phenomenon in the energy-angular correlation spectrum of the accelerated electrons for focused laser pulse. The physics underlying the bifurcating phenomenon is that both the leading electrons (the electrons ahead the electron bunch center) and the trailing electrons (behind the bunch center) can be accelerated to higher energies by intense laser pulse but with different scattering angles. These predictions have to be verified experimentally (because the presently available data are not sufficient to make such a judgment), and are of significance for further laser driven electron acceleration experiments.

ACKNOWLEDGEMENTS

This work was partly supported by the National Natural Science Foundation of China under Contracts No.10076002, No.10335030 and No. 10605010 as well as the Youth Foundation of Fudan University and the JSPS-CAS Core University Program.

REFERENCES

Badziak, J., Glowacz, S., Jablonski, S., Parys, P., Wolowski, J. & Hora, H. (2005). Laser-driven generation of high-current ion beams using skin-layer ponderomotive acceleration. *Laser Part. Beams* **23**, 401–409.

Brambrink, E., Roth, M., Blazevic, A. & Schlegel, T. (2006). Modeling of the electrostatic sheath shape on the rear target surface in short-pulse laser-driven proton acceleration. *Laser Part. Beams* **24**, 163–168.

Chen, Z., Ho, Y.K., Xie, Y.J., Zhang, S.Y., Yan, Z. & Xu, J.J., Lin, Y.Z. & Hua, J.F. (2004). Energy-angle correlation of electrons accelerated by laser beam in vacuum. *App. Phys. Lett.* **85**, 2475/3.

Fuchs, J., Antici, P., d'Humières, E., Lefebvre, E., Borghesi, M., Brambrink, E., Cecchetti, C.A., Kaluza, M., Malka, V., Manclossi, M., Meyroneinc, S., Mora, P., Schreiber, J.,

https://doi.org/10.1017/S0263034607000237 Published online by Cambridge University Press

Toncian, T., Pépin, H., Audebert, P. (2006). Laser-driven proton scaling laws and new paths towards energy increase. *Nature Phys.* **2**, 48–54.

Glinec, Y., Faure, J., Pukhov, A., Kiselev, S., Gordienko, S., Mercier, B. & Malka, V. (2005). Generation of quasi-monoenergetic electron beams using ultrashort and ultraintense laser pulses. *Laser Part. Beams* **23**, 161–166.

Hartemann, F.V. & Kerman, A.K. (2001). Classical theory of nonlinear compton scattering. *Phys. Rev. Lett.* **76**, 624–627.

Kawata, S., Kong, Q., Miyazaki, S., Miyauchi, K., Sonobe, R., Sakai, K., Nakajima, K., Masuda, S., Ho, Y.K., Miyanaga, N., Limpouch, J. & Andreev, A.A. (2005). Electron bunch acceleration and trapping by ponderomotive force of an intense short-pulse laser. *Laser Part. Beams* **23**, 61–67.

Kibble, T. W. B. (1966). Mutual refraction of electrons and photons. *Phys. Rev.* **150**, 1060/10.

Leemans, W.P., Nagler, B., Gonsalves, A.J., Tãth, CS., Nakamura, K., Geddes, E. Esarey, C.G.R., Schroeder, C.B. & Hooker, S.M. (2006). GeV electron beams from a centimetre-scale accelerator. *Nature Phys.* **2**, 696–699.

Lifschitz, AF., Faure, J., Glinec, Y., Malka, V. & Mora, P. (2006). Proposed scheme for compact GeV laser plasma accelerator. *Laser Part. Beams* **24**, 255–259.

Malka, G., Lefebvre, E. & Miquel, J.L. (1997). Experimental observation of electrons accelerated in vacuum to relativistic energies by a high-intensity laser. *Phys. Rev. Lett.* **78**, 3314/7.

Mangles, S.P.D., Walton, B.R., Najmudin, Z., Dangor, A.E., Krushelnick, K., Malka, V., Manclossi, M., Lopes, N., Carias, C., Mendes, G. & Dorchies, F. (2006). Table-top laser-plasma acceleration as an electron radiography source. *Laser Part. Beams* **24**, 185–190.

Moore, C.I., Ting, A., Jones, T., Briscoe, E., Hafizi, B., Hubbard, R.F. & Sprangle, P. (2001). Measurements of energetic electrons from the high-intensity laser ionization of gases. *Phys. Plasmas* **8**, 2481/7.

Mourou, G.A., Tajima, T. & Bulanov, S.V. (2006). Optics in the relativistic regime. *Rev. Mod. Phys.* **78**, 309–371.

Pang, J., Ho, Y.K., Yuan, X.Q., Cao, N., Kong, Q., Wang, P.X., Shao, L., Esarey, E.H. & Sessler, A.M. (2002). Subluminous phase velocity of a focused laser beam and vacuum laser acceleration. *Phys. Rev. E* **66**, 066501/4.

Quesnel, B. & Mora, P. (1998). Theory and simulation of the interaction of ultraintense laser pulses with electrons in vacuum. *Phys. Rev. E* **58**, 3719–3732.

Roth, M., Brambrink, E., Audebert, P., Blazevic, A., Clarke, R., Cobble, J., Cowan, T.E., Fernandez, J., Fuchs, J., Geissel, M., Habs, D., Hegelich, M., Karsch, S., Ledingham, K., Neely, D., Ruhl, H., Schlegel, T. & Schreiber, J. (2005). Laser accelerated ions and electron transport in ultra-intense laser matter interaction. *Laser Part. Beams* **23**, 95–100.

Salamin, Y.I. & Faisal, F.H.M. (1997). Ponderomotive scattering of electrons in intense laser fields. *Phys. Rev. A* **55**, 3678/5.

Shorokhov, O. & Pukhov, A. (2004). Ion acceleration in overdense plasma by short laser pulse. *Laser Part. Beams* **22**, 175–181.

Yin, L., Albright, B.J., Hegelich, B.M. & Fernandez, J.C. (2006). GeV laser ion acceleration from ultrathin targets: The laser break-out afterburner. *Laser Part. Beams* **24**, 291–298.